On the Prediction of Separation-Induced Transition by Coupling Delayed Detached-Eddy Simulation with γ -Transition Model

Felix M. Möller ¹, Paul G. Tucker², Zhong-Nan Wang^{2,3}, Christian Morsbach⁴, Michael Bergmann⁴

¹ Institute of Test and Simulation for Gas Turbines, German Aerospace Center (DLR), felix.moeller@dlr.de

² Department of Engineering, University of Cambridge

ABSTRACT

Powerful hybrid RANS/LES methods are gaining more attention for the prediction of transitional turbomachinery flow although the combination of these two worlds (hybrid RANS/LES and transition) is not well considered yet. Therefore, we propose a coupling of DDES and the γ -transition model. The intention behind this coupling is explained and illustrated with two test cases, namely the academic flat plate boundary layer test case with adverse pressure gradient and the T106C turbine cascade, which represent transitional flow with separation-induced transition. The fundamental behavior of the coupled DDES- γ is assessed by the flat plate test case. Further reaching analysis is done with the turbomachinery test case T106C. Both test cases helped to understand the model coupling and yield promising results for the DDES- γ model, while we showed, that the fully-turbulent DDES failed to capture relevant features of the transitional flow for low free-stream turbulence.

KEYWORDS

Hybrid RANS/LES, Delayed Detached-Eddy Simulation, γ -Transition Model, Separation-Induced Transition, Turbine Cascade

NOMENCLATURE

Variables		Abbreviations			
$ \begin{array}{c} l \\ t \\ c_{ax} \\ s \\ f \\ k \\ c_f \\ \gamma \\ M_{is} \end{array} $	length scale time scale axial chord length pitch frequency turbulent kinetic energy friction coefficient intermittency factor isentropic Mach number	RANS LES HRL DDES FT FSTI SLS	Reynolds-averaged Navier-Stokes large-eddy simulation hybrid RANS/LES delayed detached-eddy simulation fully turbulent free-stream turbulence intensity sub-grid length scale		
$\stackrel{\zeta}{x},y,z$	total pressure losses streamwise, wall-normal and	Subscri	pts		
$u, v, w \\ \Delta_x^+, y^+, \Delta_z^+$	spanwise coordinate respective velocity components respective non-dimensional cell sizes	$ \Box_{\text{ref}} \\ \Box_{\text{exp}} \\ \Box_{\text{mod}} \\ \Box_{\text{res}} $	reference quantity experimental quantity modelled quantity resolved quantity		

1

³ College of Engineering and Physical Sciences, University of Birmingham

⁴ Institute of Propulsion Technology, German Aerospace Center (DLR)

INTRODUCTION

The accurate prediction of transitional turbomachinery flows is a challenging discipline for state-of-the-art CFD methods. Established Reynolds-averaged Navier-Stokes (RANS) models in combination with correlation-based transition models have been utilized for a long period of time and are considered as capable methods for moderate flow conditions like attached flow, occurring at the design point of a turbomachine. There exists a large number of successful demonstrations for RANS models predicting transitional flows, but yet, authors also report deficiencies and limitations like modelling separation-induced transition [Nürnberger and Greza (2002)], treating crossflow instabilities and a non-Galilean invariant formulation [Langtry and Menter (2009)] or the dependency of empirical correlations predicting the transition process [Pasquale et al. (2009)]. While RANS methods fail at off-design conditions with massive separation [Langtry et al. (2006)], the coincidence with laminar-to-turbulent transition represents an even bigger challenge. The arising demand of gaining more insights from CFD results and the increasing desire of analyzing unsteady effects in turbomachinery flows pushes RANS approaches to their limits, or even they fail to predict relevant flow features [Tyacke et al. (2013)].

The noticeably more expensive large-eddy simulation (LES) method is an approach to deal with the abovementioned conditions since the modelling amount is reduced to a minimum and most of the relevant scales are spatially and temporally resolved. This increased resolved amount of turbulent stresses promotes the prediction of transitional flows without an additional transition model. Due to the dependency between the Reynolds number and required mesh points, LES is still limited to lower Reynolds numbers due to the computational effort [Tucker (2013)].

A popular compromise between affordable RANS models and accurate LES methods are hybrid RANS/LES (HRL) approaches. Especially for separated flows, occurring at off-design conditions, the DES method, initially proposed by Spalart et al. (1997), is widely used with convincing results. During the past decades many developments helped to mitigate issues such as grid-induced separation [Menter et al. (2003)], caused by modelled-stress depletion [Spalart et al. (2006)], and the grey-area problem [Strelets (2001)], which is understood as a delayed transition from modelled to resolved content. New model versions like the delayed detached-eddy simulation (DDES) [Spalart et al. (2006)] and vorticity-based sub-grid length scale approaches [Chauvet et al. (2007); Mockett et al. (2015); Shur et al. (2015)] have been proposed to face the aforementioned issues. The main focus of these approaches has always been fully turbulent flows.

The simulation of transitional flows with DES methods is a rarely considered field in the past, while Wang et al. (2012) already mentioned the aspect of applying their introduced RANS transition model in the DES framework. Exemplarily publications regarding the coupling of DES and a transition model (in the following we will generally refer to it as DES-Tr) exhibit a big variety of how to treat transitional flows with DES. Sørensen et al. (2011) combined the DES with a k- ω SST basis model and a correlation-based γ - Re_{θ} transition model. Alam et al. (2013) proposed a new transition-sensitive dynamic HRL (TDHRL) model. It is based on the k-k- ℓ - ℓ model by Walters and Cokljat (2008) and extended for DDES applications. Hodara and Smith (2017) presented another way to run DES-Tr while they combined the γ - Re_{θ} model with a localized dynamic kinetic energy model (LDKM) [Kim and Menon (1999)]. Xiao et al. (2019) considered the challenging hypersonic flow past the Orion capsule and therefore applied a three-equation k- ω - γ DDES model introduced by Wang and Fu (2009). Yin et al. (2021) utilized an adaptive ℓ - ω DDES model motivated by the desire of a hybrid modelling approach without

an additional transport equation for the intermittency factor. Hence, the transition process is treated by the hybrid model inherently. The large number of different approaches enabling DES versions to predict transitional flows illustrates the growing interest for this research field but yet a trend about the 'right' concept is not clear. All presented DES-Tr approaches have shown better results in comparison to fully turbulent DES or RANS computations.

Generally, DES methods are applied for configurations where detached flows are expected, which means a separation-induced transition is likely to appear in case of low free-stream turbulence intensity (FSTI) inflow, which is why we first focus on this transition type for now with test cases experiencing low FSTI. Further transition types such as bypass or wake-induced transition will be objectives of future work.

METHODOLOGY

Before we assess obtained numerical results, we introduce the applied basis models and explain the intention behind the coupling approach. Followed by a brief introduction of the utilized solver and our assessment approach to classify obtained results.

Basis Models

It is our intention to keep the coupled approach as simple as possible since fully turbulent DES approaches already contain a variety of switches and 'decision makers'. Hence, we strive for a moderate additional workload and plain model design. The k- ω SST turbulence model in its version of Menter et al. (2003) constitutes the foundation of the applied DDES approach originally proposed by Travin et al. (2002). This well-known RANS model consists of two transport equations for the turbulent kinetic energy k and the turbulent dissipation rate ω . The destruction term in the k-transport equation can be expressed as $D_k = \beta^* \rho \omega k$. The definition of the turbulent length scale $l_{\rm RANS} = k^{1/2}/(\beta^* \omega)$ allows a reformulation based on $l_{\rm RANS}$

$$D_k = \frac{\rho k^{3/2}}{l_{\text{RANS}}} \tag{1}$$

which plays an important role for the model hybridization. It is, in fact, the only 'manipulation' to change the RANS approach to a HRL one. This is realized by replacing $l_{\rm RANS}$ in Eq. (1) with a newly introduced DDES length scale

$$l_{\text{DDES}} = \min\left((1 - f_d) l_{\text{RANS}} + f_d C_{\text{DES}} \Delta_{\text{SLS}}, l_{\text{RANS}} \right) \tag{2}$$

resulting in a new form of the destruction term

$$D_k = \frac{\rho k^{3/2}}{\min\left((1 - f_d)l_{\text{RANS}} + f_d C_{\text{DES}} \Delta_{\text{SLS}}, l_{\text{RANS}}\right)}$$
(3)

where f_d is Spalart's shielding function [Spalart et al. (2006)]. Eventually, we introduce the utilized sub-grid length scale (SLS) approaches. The originally proposed $\Delta_{\rm SLS} = \Delta_{\rm max} = \max{(\Delta_x, \Delta_y, \Delta_z)}$ approach [Spalart et al. (1997)] has an issue with reasonable switching from RANS to LES branch, hence, the transition from modelled to resolved content is delayed or at least highly grid dependent. Newer vorticity-based approaches do not only consider the cell sizes, but also actual flow physics by incorporating information from the vorticity field. The $\Delta_{\rm SLA}$ approach by Shur et al. (2015) which is an extension of the $\tilde{\Delta}_{\omega}$ approach by Mockett et al. (2015) are popular vorticity-based model versions. The SLA extension was proposed

to include a more kinematically motivated measurement for the initial shear layer where the grid anisotropy does not play the dominant role [Shur et al. (2015)]. This ensures an even faster transition from modelled to resolved content in developing shear layers. Investigations on the Volino series will compare all three length scale approaches ($\Delta_{\rm max}$, $\tilde{\Delta}_{\omega}$, $\Delta_{\rm SLA}$), while simulations of the T106C test case are focused on the $\Delta_{\rm SLA}$ approach.

Bearing in mind the motivation of having a plain DES-Tr approach we decide to focus on the correlation-based one-equation γ -transition model proposed by Menter et al. (2015). The intermittency factor γ is determined by an individual transport equation. The model is derived from the γ - Re_{θ} -model which consists of two transport equations, where the Re_{θ} -transport equation is replaced with an algebraic approach based on local variables. Another strength of the γ -model is its Galilean invariant formulation which is advantage in contrast to the γ - Re_{θ} -model. We do not include further detailed equations here since the underlying functions and switches are well-explained by Menter et al. (2015).

Coupled DDES- γ Model

Basically, there are three possible scenarios of interest for separated flows, potentially treated with DDES: a laminar separation with laminar reattachment, laminar separation with turbulent reattachment and turbulent separation with turbulent reattachment [Yanaoka et al. (2007)]. As said, we focus on separation-induced transition which addresses laminar separation with turbulent reattachment. Laminar separation with laminar reattachment is unlikely in turbomachinery since this would require very low FSTI to omit the stimulation of instabilities initiating transition in the separated shear layer. Turbulent separation with turbulent reattachment is a prominent mechanism in turbomachinery, but, assuming laminar inflow, this would involve bypass transition prior to the separation which is not objective of this work.

Before talking about the DDES- γ coupling and interactions, it is indispensable to introduce the redefined k-transport equation for intended RANS applications by Menter et al. (2015)

$$\frac{\partial}{\partial t}(\rho k) + \frac{\partial}{\partial x_i}(\rho u_j k) = \tilde{P}_{k,\text{trans}} + P_k^{\text{lim}} - \tilde{D}_k + \frac{\partial}{\partial x_i} \left((\mu + \sigma_k \mu_t) \frac{\partial k}{\partial x_i} \right)$$
(4)

to incorporate the effect of γ on the applied turbulence model. This is facilitated with a modified production term $\tilde{P}_{k,\mathrm{trans}} = \gamma \tilde{P}_k$ and destruction term $\tilde{D}_k = \max{(\gamma,0.1)}D_k$. Further, Menter et al. (2015) included an additional production term P_k^{lim} which will be addressed later on. Generally speaking, $\gamma = 0$ states a laminar flow and $\gamma = 1$ denotes a fully turbulent flow. Thus, the turbulent production of k in Eq. (4) is reduced to zero for laminar flows meanwhile the k-destruction is also reduced but guaranteed to be at least 0.1 of the original D_k . Hence, the amount of modelled turbulent kinetic energy is pruned by γ .

In the coupled DDES- γ model, the new destruction term, incorporating both model branches, is designed as follows:

$$\tilde{D}_{k,\text{trans}} = \max\left(\gamma, 0.1\right) \frac{\rho k^{3/2}}{l_{\text{DDES}}} \tag{5}$$

In first instance, this re-formulated $\tilde{D}_{k,\mathrm{trans}}$ looks contradictory. γ -values between 0.1 and 1.0 try to reduce the destruction term while for $\Delta_{\mathrm{SLS}} < l_{\mathrm{RANS}}$ (see the definition of l_{DDES} in Eq. (2)) the value of $\tilde{D}_{k,\mathrm{trans}}$ is increased via smaller l_{DDES} values in comparison to l_{RANS} . Both branches act with the same intention: reducing the modelled amount of turbulent kinetic energy. But the initial situation is entirely different. The original γ -model is designed for laminar flow

conditions. This means the amount of modelled turbulent kinetic energy is close or equal to zero and γ prevents the model to determine premature modelled content by hindering any production whereas destruction is maintained at least $10\,\%$ to ensure a low level of μ_t . On the other hand, the original fully turbulent DES model was designed for flow conditions where a big amount of modelled turbulent kinetic energy is already apparent. An increase of the destruction term results in the reduction of modelled content while resolved content is caught. Both attributes of the respective models should be maintained to keep their applicability in originally intended flow conditions. For the joint DDES- γ approach, the different model branches and intentions do to not obstruct each other which will be confirmed in our result sections.

The mentioned additional production term P_k^{\lim} (cf. Eq. (4)) requires separate attention. So far, all terms were accepted to work properly also for the coupled DDES- γ , but P_k^{\lim} does not. Menter et al. (2015) found that the original γ -model including basis SST model struggles with the proper generation of modelled turbulent kinetic energy when the flow separates laminar and transition occurs in the shear layer. Therefore, they introduced this additional term to add modelled turbulent kinetic energy in the separated shear layer and, thus, reduce the development length of turbulence by the model. This additional term is comparable to the model behavior of the γ -Re $_{\theta}$ -model by Menter et al. (2006), whereas for the γ -Re $_{\theta}$ -model the accelerated transition to a turbulent state is realized by local γ values greater than unity. In fact, this additional modelled turbulent kinetic energy is undesired for DDES- γ simulations since it adds artificial damping to the system and, thus, prevents the determination of resolved content. This is contradictory to the main goal of DDES- γ whereby the transitional process should mainly be captured by resolved stresses. For turbulent boundary layers, $P_k^{\rm lim}$ is designed to disappear [Menter et al. (2015)] and for occurring bypass transition, this source term will not add any turbulent kinetic energy either. Hence, we propose to remove this additional source term for the application of DDES- γ , bringing us to a modified k-transport equation including the γ impact by $\tilde{P}_{k,\text{trans}}$ and $D_{k,\text{trans}}$

$$\frac{\partial}{\partial t}(\rho k) + \frac{\partial}{\partial x_j}(\rho u_j k) = \tilde{P}_{k,\text{trans}} - \tilde{D}_{k,\text{trans}} + \frac{\partial}{\partial x_j} \left((\mu + \sigma_k \mu_t) \frac{\partial k}{\partial x_j} \right)$$
 (6)

whereas all other terms are unaffected. Consequently, we applied the original ω - and γ -transport equations and the modified Eq. (6) as a set of equations to couple Menter's SST model and γ -model and show the effectiveness of a hybrid approach to predict separation-induced transition.

Numerical Solver

All simulations have been carried out with the DLR in-house solver TRACE¹ which is developed at the Institute of Propulsion Technology in the Department for Numerical Methods. The utilized branch of TRACE is a density-based cell-centered finite-volume solver designed for turbomachinery applications. Presented numerical results, unless marked otherwise, were solved by the finite volume method with a 2nd-order accurate spatial discretization scheme. Additionally, we applied the proposed numerical blending function by Strelets (2001). For the DDES method, fully upwind schemes behave too dissipative and suppress potential resolved content from the LES branch. Therefore, a blending between central fluxes (active for LES branch) and upwind fluxes (active for RANS branch) is recommended. The required convective time scale to control the blending function is specified for each test case separately. A 3rd-order explicit Runge-Kutta method is applied for temporal discretization.

¹TRACE User Guide, https://trace-portal.de/userguide

Assessment approach

To show the feasibility of predicting separation-induced transition by DDES- γ is the main motivation of this work. Furthermore, not only showing a proper working DDES- γ model but also the comparison to competing approaches such as

- numerical LES reference data
- experimental reference data (if data is available for considered variable)
- RANS data (labeled as RANS- γ or RANS- γ - Re_{θ})
- fully turbulent DDES data (labeled as DDES-FT)

is of big interest. Additionally, for the Volino series, we present results for the plain coupling of DDES and γ -model including the $P_k^{\rm lim}$ -term (in the following referred to as DDES- γ - $P_k^{\rm lim}$). This will emphasize the positive effect of our proposed coupling without the additional production term. The comprehensive comparison helps assess numerical results and the benefits of DDES- γ .

VOLINO SERIES

This flat plate test case was designed by Volino and Hultgren (2000) to reproduce the streamwise adverse pressure gradient on the suction side of the PAK-B turbine blade, experimentally first investigated by Qiu and Simon (1997). Since we are focusing on separation-induced transition in this paper, we consider the low FSTI (= 0.2%) case with a laminar boundary layer prior to separation and a Reynolds number of 50'000. The reference length applied for normalization is equal to the considered suction surface length $l_{\rm ref, \, exp} = 0.2075 \, {\rm m}$. The reference velocity $u_{\rm ref, \delta_{99.5, exp}} \approx 4.23 \, {\rm m/s}$ is determined at the boundary layer edge at measurement station 13 (illustrated in Fig. 1).

Fig. 1 shows the general test case configuration and flow regions for the test section. Based on their experimental resolution (number of measurement points), Volino and Hultgren (2000) found that the separation location does not vary for different flow conditions and was measured at $x/l_{\rm ref} \approx 0.65$. The subsequent, separated shear layer is characterized by growing instabilities which trigger the transition after exceeding a certain threshold. For the abovementioned operating point, the transition was determined at $x/l_{\rm ref} = 1.0$. Fig. 1 shows the experimental measurement stations and clarifies that reattachment does not occur within the experimental test section. The DDES has to deal with two main regions of this test case. First, the attached

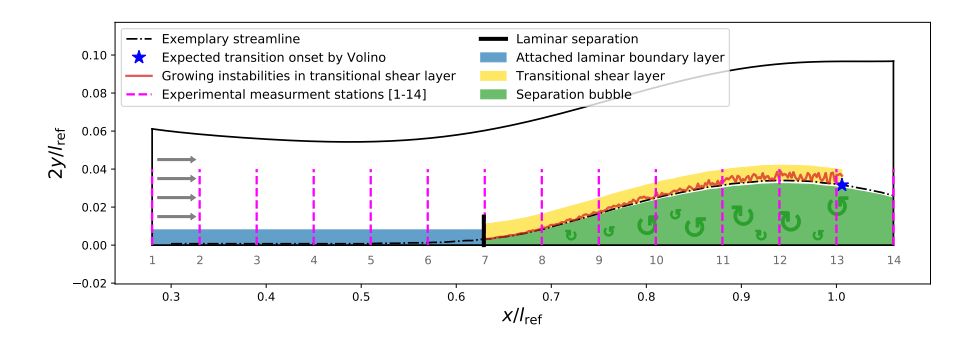


Figure 1: Schematics of Volino series depicting the relevant regions for Re = 50'000 and FSTI 0.2%. Experimental measurement stations marked by index.

laminar boundary layer must be kept laminar by the underlying transition model to prevent unphysical, premature modelled content by the turbulence model. Further, in the separated region, we want the unsteady branch of DDES to treat the transition and rather resolve this process, provided that a sufficient mesh resolution is available. Generally, this process is disturbed when modelled turbulent content is already present prior to separation or additionally added in the separated shear layer (which is more likely to occur for higher FSTI cases). That means an increased damping by modelled scales hinders the model to resolve the transitional process accurately. Based on this test case, we start the assessment of our DDES- γ model and its predictive behavior.

Numerical Setup

The contour of the upper inviscid wall is generated following Suzen et al. (2003). The spanwise extent is defined by $50\,\%$ of the computed separation bubble size with RANS- γ . As a starting point for the mesh design, we consider investigations by Menter et al. (2015) who also simulated the Volino series. These investigations are based on pure RANS configurations, hence, a 2D mesh was proposed with a resolution of 312×70 nodes for the operating point of interest. As Menter et al. (2015), we also extended the computational domain for the test section up to $x/l_{\rm ref}=1.6$. Additionally, we added a sponge zone until $x/l_{\rm ref}=2.08$ to reduce downstream effects from the exit panel. The mesh resolution in the test section is realized comparable to the Menter et al. (2015) RANS setup as summarized in Tab. 1.

Table 1: Overview of applied meshes (streamwise \times wall-normal \times spanwise).

	Test section	Sponge zone	Total number of cells	$\Delta x_{\rm max}^+$	y_{max}^+	$\Delta z_{\rm max}^+$
LES	$460 \times 70 \times 64$	$15 \times 70 \times 64$	2'128'000	14.44	0.74	14.78
DDES	$300\times70\times42$	$15\times70\times42$	926'100	22.21	0.74	22.58
RANS	$300\times70\times1$	$15\times70\times1$	23'800	19.38	0.65	-

The static exit pressure was determined by computational iterations until the derived exit mass flow from experimental reference data was fitted well. Regarding the entry, we derived a 1D profile matching all experimentally measured values at station 1. In accordance with the experimental flow conditions, we prescribed FSTI = 0.2% and a turbulent length scale of $l_{\rm RANS} = 0.01$ m which ensures a laminar boundary layer prior to the separation. The boundary condition for the γ -model is well-described in Menter et al. (2015). At the inlet we constantly prescribe $\gamma = 1$ while at the wall we have a zero normal flux boundary condition. Both settings are recommended by Menter et al. (2015) and also utilized for their previously introduced two-equation γ - Re_{θ} -model in Menter et al. (2006).

For the unsteady simulations we define the convective time scale $t_c = l_{\rm ref}/u_c$ which is used by the DDES setup for central-upwind-blending. We further use t_c for normalization. The characteristic velocity u_c is determined at the boundary layer edge at station 13, resulting in a convective time scale $t_c = 4.9 \cdot 10^{-4} \, \rm s$. The physical time step is defined as $\Delta t/t_c = 3.11 \cdot 10^{-5}$ for the LES setup and DDES setups. The defined time steps ensure a CFL number below 1.

Results

First, the friction coefficient along the lower wall in the test section is illustrated in Fig. 2. The last experimental station ($x/l_{\rm ref} = 1.06$) is depicted flipped about the x-axis (original value

was positive).² The moderate backflow after separation at $x/l_{\rm ref} \approx 0.63$ with a subsequent sharp c_f -drop at $x/l_{\rm ref} \approx 1.0$ is a typical c_f trend for separation-induced transition. All three subplots include experimental reference data, numerical LES reference and RANS results. The LES reference shows good agreement for separation and transition onset location with experimental data. Further, it becomes clear, that the steady RANS- γ model is not capable to predict the accurate transition process, meaning an overprediction of the separation bubble size and a premature increase of reversed flow indicating earlier transition onset.

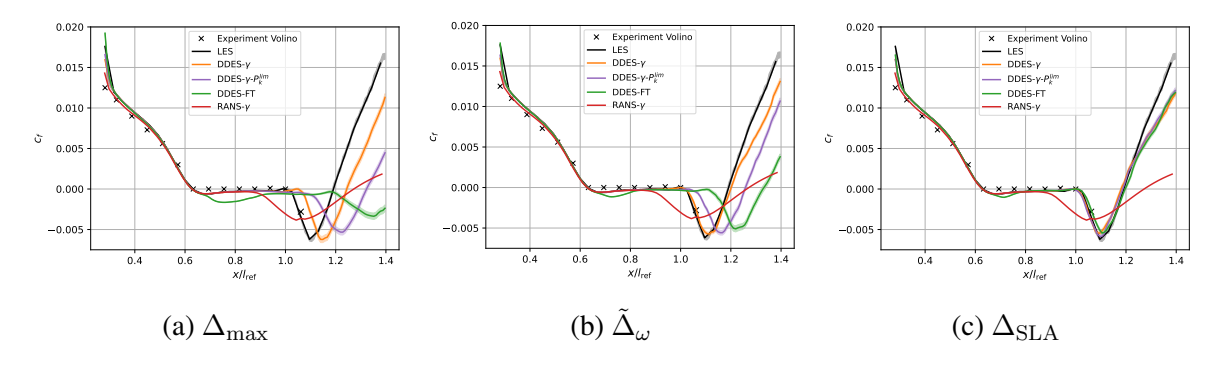


Figure 2: Friction coefficient along the lower wall for all three Δ_{SLS} approaches including 95% confidence interval for the unsteady simulations.

For all unsteady simulations, we show the corresponding error band. Bergmann et al. (2021) described a method for determining the initial transient and mean error of a given time signal. Removing this initial transient yields the effective number of throughflows (for LES simulation: $t/t_c=417$ and DDES simulations: $t/t_c=57-87$). The depicted error bands in Fig. 2 show a very small range of uncertainty which illustrates the statistical convergence of the LES and DDES results.

The effectiveness of coupling DDES and the γ -model is shown for each sub-grid length scale approach. For Δ_{\max} (cf. Fig. 2a), the fully turbulent DDES simulation predicts a delayed transition onset with an over-estimated separation bubble. A plain coupling of DDES and the γ -model (including P_k^{\lim}) at first improves the model behavior, but there is still a bigger discrepancy to numerical reference data. The deactivation of the additional production term P_k^{\lim} yields almost identical results in comparison to LES. This trend is confirmed by the $\tilde{\Delta}_{\omega}$ length scale approach (cf. Fig. 2b), while the proposed model coupling DDES- γ shows best results and coincides with the LES reference data. For the extended length scale approach Δ_{SLA} (cf. Fig. 2c), all computational DDES results collapse to LES reference data. This special behavior for Δ_{SLA} is explainable with the original model intention to act like an implicit LES in the shear layer. Due to the fine mesh resolution (summarized in Tab. 1), the effect of sub-grid eddy-viscosity is reduced to a minimum for Δ_{SLA} , which leads to an almost identical behavior of all three DDES simulations - also favored by identical boundary layer profiles prior to the separation. Results of the T106C will show that this is not a general model behavior, but specific for the Volino series. In the following Volino series analysis, we focus on the $\tilde{\Delta}_{\omega}$ approach.

The transition process can also be clarified by evaluating the wall-normal resolved turbulent kinetic energy profiles. The maximum value at each station is depicted in Fig. 3. Volino (2002) reported a transition onset at $x/l_{\rm ref}=1.0$ which is consistent with our LES data. The trend

²Personal correspondence with Prof. Volino

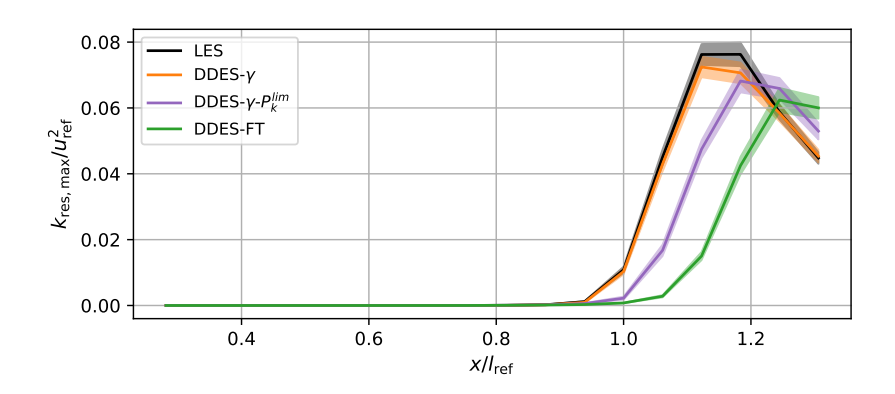


Figure 3: Maximum resolved turbulent kinetic energy along defined x-stations including 95% confidence interval.

from the c_f plot in Fig. 2 is confirmed by evaluating the maximum resolved turbulent kinetic energy. Deviations of the transition start and end location from the LES are reduced with DDES- γ (almost identical results), while the fully turbulent approach and even a simple coupling of DDES and γ -model including $P_k^{\rm lim}$ fail to predict the transitional process in an accurate manner.

An explanation for these different results can be given by analyzing the contour plots of modelled turbulent kinetic energy, shown in Fig. 4. It becomes clear, that the fully turbulent approach (cf. Fig. 4a) prematurely produces modelled turbulent kinetic energy in the initial separated shear layer. Thus, growing instabilities are damped immediately by modelled content resulting in a delayed transition onset. That is because no underlying transition model prevents the production of modelled turbulent kinetic energy. Additionally, profiles of the total turbulent kinetic energy $k_{\rm tot}$ are visualized. It becomes clear, that premature modelled content prevents resolved scales and the overall turbulence level is lower and shifted downstream. This is the reason, why the separation bubble size is increased for DDES-FT which is in good agreement with trends in Fig. 2b and Fig. 3. Improvements are apparent when coupling the DDES with γ -model including P_k^{\lim} (cf. Fig. 4b), meaning the modelled content in the initial separated shear layer is effectively reduced. But in the region of interest, where the transition onset takes place, there is still undesired modelled turbulent kinetic energy which damps relevant instabilities - also resulting in delayed transition. This is because the transition model activates the additional production term $P_k^{\rm lim}$ from $x/l_{\rm ref} \approx 0.8$. The deactivation of $P_k^{\rm lim}$ is depicted in Fig. 4c. The modelled content is shifted further downstream to the turbulent region, while the separated, transitional shear layer is not affected by any damping. The circumstances prior to separation are identical for all simulations. Due to very low FSTI (0.2%) and a short upstream length between inlet and separation, the attached, laminar boundary layer does not remarkably change in this region. It is the separated shear layer, which triggers relevant instabilities for this case. The amount of modelled content from the turbulence model is obviously linked to the development of resolved ones (cf. Fig. 3). If the underlying turbulence model produces too much modelled turbulent kinetic energy, the DDES model is incapable of resolving the transition process accurately.

To better understand the interaction between the γ -model and Spalart's shielding function f_d , we compare these two values exemplarily for DDES- γ in Fig. 5. It becomes clear, that γ remains almost constant at unity in the free-stream. In the laminar boundary layer, γ is reduced to zero, whereas the transition model begins to switch from zero to unity in the separated shear

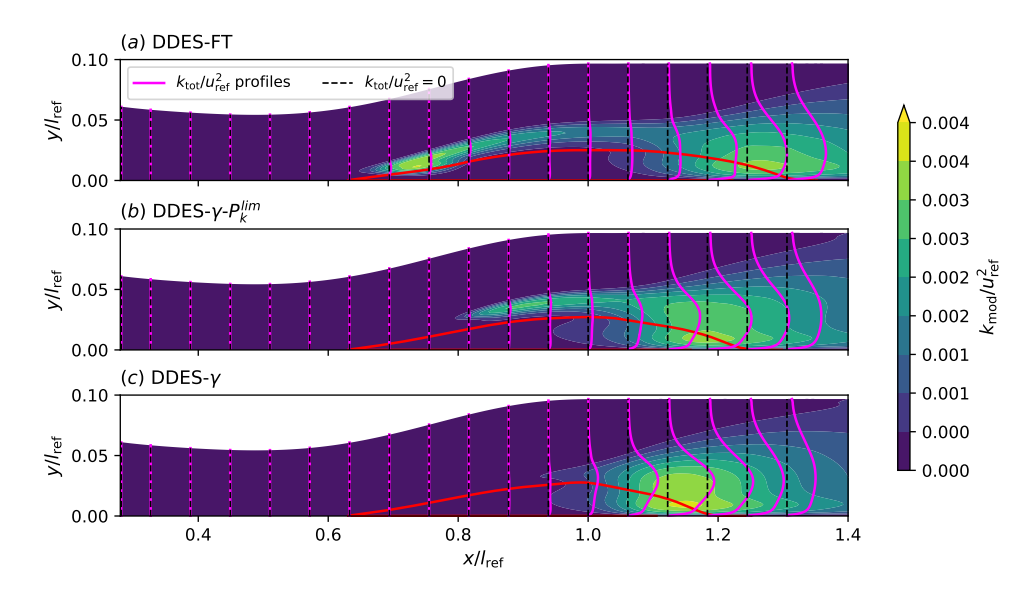


Figure 4: Time-averaged modelled turbulent kinetic energy contour including profiles of total turbulent kinetic energy at introduced stations. Separation bubble approximated by the shear layer border $u/u_{\rm ref}=0$ (red line).

layer at $x/l_{\rm ref} \approx 0.8$. On the other hand, the shielding function f_d is almost constantly zero from the beginning of the domain. Artifacts at the upper wall may be neglected since this is the interaction with the inviscid wall. The shielding function detects the border of the boundary layer from $x/l_{\rm ref} \approx 0.4$, which switches f_d to unity in this region. This allows for a comparison between $l_{\rm RANS}$ and $\Delta_{\rm SLS}$, hence, an activation of LES-mode. Focusing on the the free-stream, we see no negative interference of γ and f_d . $\gamma=1$ maintains the prescribed free-stream turbulence and $f_d=0$ keeps the model in RANS-mode. We discussed the re-defined destruction term (cf. Eq. (5)) in the methodology section. The illustration of γ - and f_d -profiles supports our point of view. In the initial part of the separated shear layer, $\gamma=0$ keeps modelled turbulent kinetic energy to a minimum, which enables the development of resolved scales. Further downstream, where the transition model detects a transitional process, $f_d=1$ enables the LES-mode, which, again, recduces undesired modelled turbulent kinetic energy.

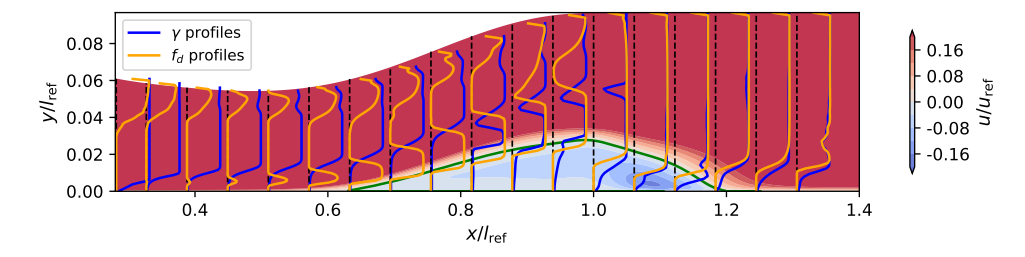


Figure 5: Comparison of γ - and f_d -profiles for DDES- γ . Contours illustrate the normalized flow field. Separation bubble approximated by the shear layer border $u/u_{\text{ref}} = 0$ (green line).

Eventually, in Fig. 6, we analyze selected values along an extracted streamline (exemplarily depicted as black dashed line in Fig. 1), which lies within the initially laminar boundary layer, to further illustrate the coupling of DDES and γ -model. The active γ -model in DDES- γ prior to the separation (cf. Fig. 6a) has direct impact on the production of eddy-viscosity (cf. Fig. 6b)

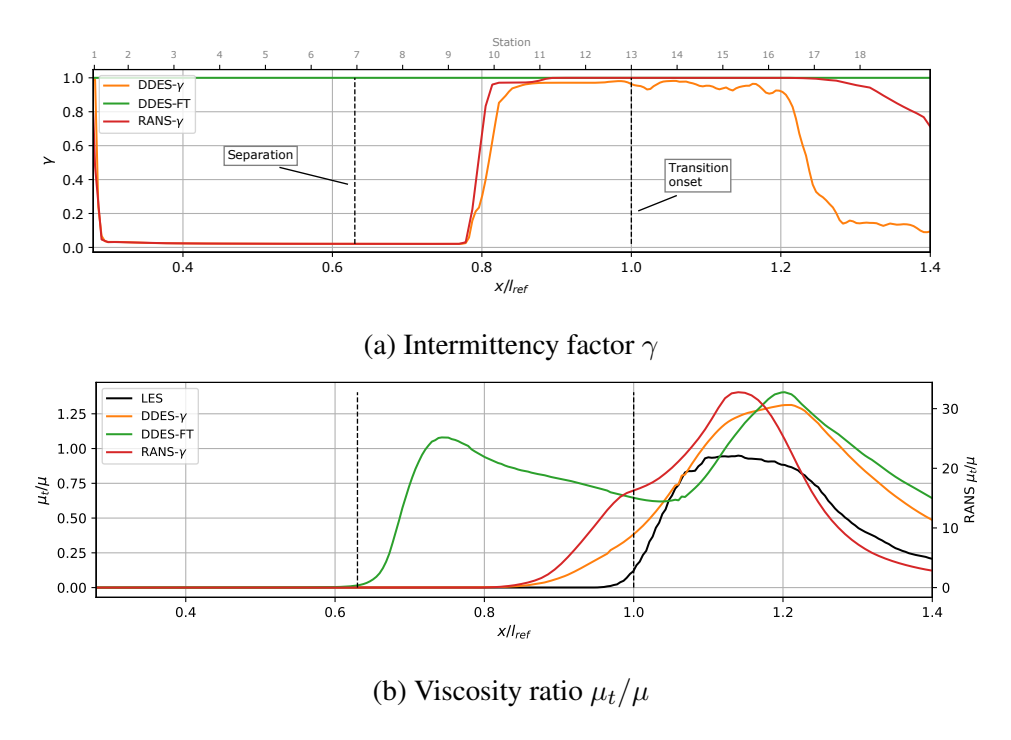


Figure 6: Selected variables along extracted streamline depicted in Fig. 1. In (b), left y-axis relates to DDES/LES simulations and right y-axis relates to RANS.

by keeping it to a minimum. The absence of a transition model facilitates an immediate increase of μ_t in the initial part of the separated shear layer for DDES-FT which is not predicted by any other computation. A subsequent increase of μ_t in the transitional region at $x/l_{\rm ref} \approx 1.0$ is in good agreement with the LES reference.

The comparison of numerical results with the Volino series yield promising results. While we see beneficial behavior of the coupled DDES- γ approach, we learnt, that fully turbulent DDES is not capable of predicting separation-induced transition correctly. This canonical test case has been a good starting point to evaluate the coupling of DDES and the γ -model. Findings from this test case help to start our analysis of the T106C turbine cascade.

TURBINE CASCADE T106C

We investigate the low-pressure turbine cascade T106C which was designed by MTU Aero Engines and comprehesively investigated within the *High-Order CFD Methods* workshop with laminar inflow conditions (FSTI = 0%). The focussed operating point is Re = 80'000 and $Ma_{2,is} = 0.65$. In combination with laminar inflow, separation-induced transition and a potentially open separation bubble (depending on the applied model and defined boundary conditions) occur on the suction side of the turbine blade. A comparable operating point was experimentally measured by Michálek et al. (2012). Their low-turbulence setup yields FSTI = 0.9%. This data will serve as an orientation. The main focus is the numerical comparison of RANS, DDES and LES.

Numerical Setup

An overview of the computational domain and boundary conditions is sketched in Fig. 7. For all unsteady setups, the inflow turbulence and turbulent length scale are set equal to zero.

While RANS models are not calibrated for zero free-stream turbulence, we prescribe a minimum inflow turbulence level of 1% and an inflow turbulent length scale equal to $1\times 10^{-4}\,\mathrm{m}$. This numerical setup has been comprehensively analyzed by Morsbach and Bergmann (2020) and Bergmann et al. (2021). Based on their findings, we defined a span extent of z/c=0.3.

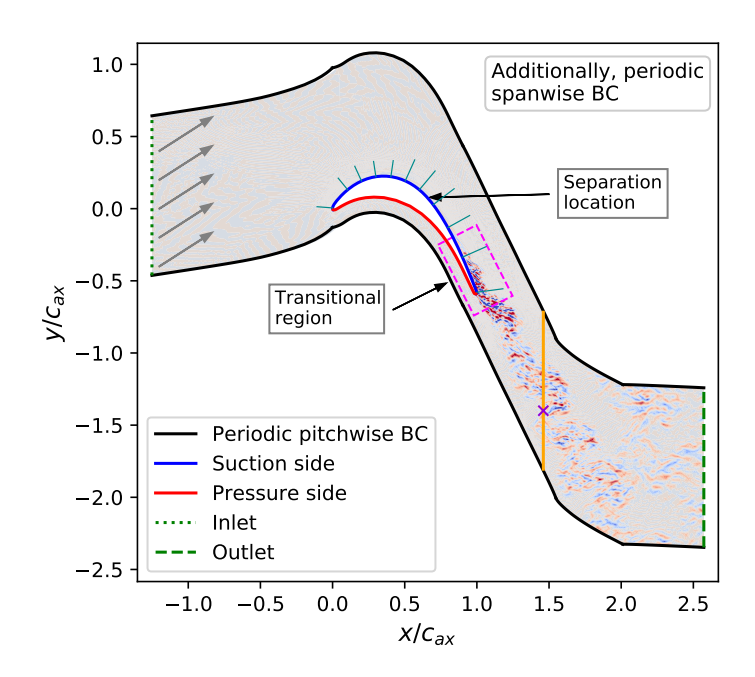


Figure 7: Schematics of computational domain for T106C including exemplarily wall-normal boundary layer cuts (cyan) and considered wake position (orange). Background contour shows instantaneous streamwise vorticity field for LES reference data.

The LES reference simulation was conducted on a sufficiently fine grid (analyzed by Bergmann et al. (2021)), summarized in Tab. 2 and in the following referred to as LES. Preceding studies yield a coarser mesh version for which the LES model was not capable to predict the flow accurately (we will also include these results labeled as LES-underresolved). We used this mesh version (also summarized in Tab. 2) to assess the performance of DDES. As we run the explicit Runge-Kutta method, again, we need to define a sufficient time step size to meet CFL < 1. The resulting time step for the DDES simulations is $\Delta t/t_c = 3.64 \cdot 10^{-5}$. To determine the convective time, we used the chord length c and the averaged outlet velocity $|\overline{u_{outlet}}|$ as characteristic velocity.

Table 2: Overview of T106C grid setups and non-dimensional cell sizes at suction side.

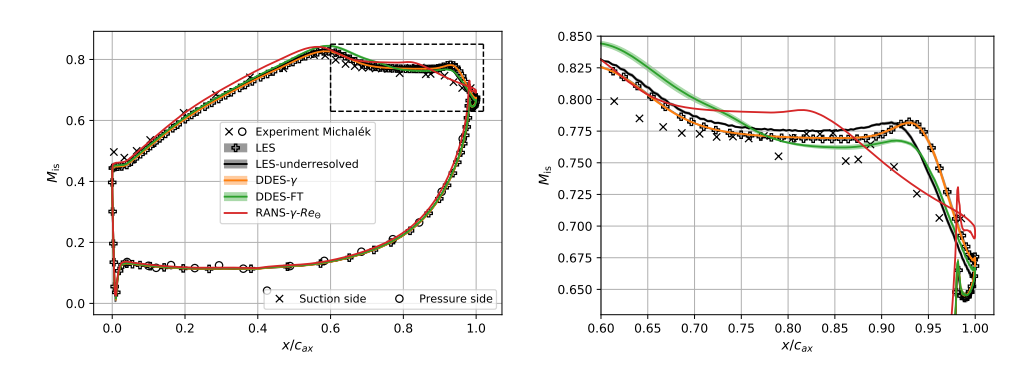
	Total number of cells	$\Delta x_{\mathrm{max}}^+$	$y_{\rm max}^+$	$\Delta z_{ m max}^+$
LES	14'822'190	17.12	0.31	16.99
DDES- γ , DDES-FT & LES-underresolved	4'391'760	25.81	0.47	25.61

In contrast to the Volino series, we focus on the Δ_{SLA} -approach. We learnt, that this more sophisticated approach shows no big differences for the specific Volino series test case, but

the T106C results illustrate differences between fully turbulent and transitional model. Furthermore, for better overview, we avoid showing additional results for DDES- γ - P_k^{\lim} to keep a better focus on our proposed model version DDES- γ . The effect of the additional production term has been assessed for the Volino series before.

Results

A first overview of computational results is given by the isentropic Mach number along the blade surface in Fig. 8. Results for the pressure side are almost identical for all numerical simulations, whereas on the suction side, we see differences especially in separation and transition region (marked by dotted box and illustrated in Fig. 8b). For RANS, we further consider the coupling of the Menter-SST model and γ -Re $_{\theta}$ -model (implemented in the version of Langtry and Menter (2009)). The coupling with the proposed γ -model did not achieve convergence for the RANS setup and additionally, the γ -Re $_{\theta}$ -model is commonly used to conduct transitional RANS simulations in turbomachinery context. We see that the RANS- γ -Re $_{\theta}$ -model also yields



(a) Overview. Dashed rectangle marks (b) Zoomed in on the suction side in sepzoomed region in (b). arated and transitional region.

Figure 8: Isentropic Mach number along the blade surface including 95% confidence level for the unsteady simulations. Shown every 5^{th} point for LES reference data.

acceptable results in comparison with the unsteady simulations. The fully turbulent DDES simulations shows higher Mach numbers in the initial part of the separation with a faster drop to a Mach plateau on lower level. The DDES- γ model follows the LES reference while the LES-underresolved on the same mesh shows deviations with a premature Mach number drop. Eventually, DDES-FT and LES-underresolved coincide at $x/c_{ax}\approx 0.93$. The peak between $x/c_{ax}=0.9-0.95$ only predicted by unsteady simulations corresponds to a secondary separation bubble which is not captured by the experiment and RANS- γ - Re_{θ} .

In Fig. 9, we illustrate the friction coefficient along the suction surface. All unsteady simulations show general good agreement with LES (cf. Fig. 9a) except for RANS- γ - Re_{θ} which shows higher c_f values close after the leading edge, resulting in a premature separation and general failure to predict the separation-induced transition. The zoomed view in Fig. 9b reveals relevant differences prior to the separation and in the transitional region. The abovementioned secondary separation bubble is identifiable in the c_f trend where the intensity of forward flow is directly linked to peak level in Fig. 8. Further, it becomes clear, that DDES- γ follows LES which is worth mentioning since it was computed on a coarser mesh. However, in contrast to previous Volino series c_f trends (cf. Fig. 2a or Fig. 2b), the fully turbulent simulation does not

show a delayed but a premature transition, closer to the LES-underresolved result on the same coarse mesh. To explain this trend, we focus in the pre-separation region. While for the Volino

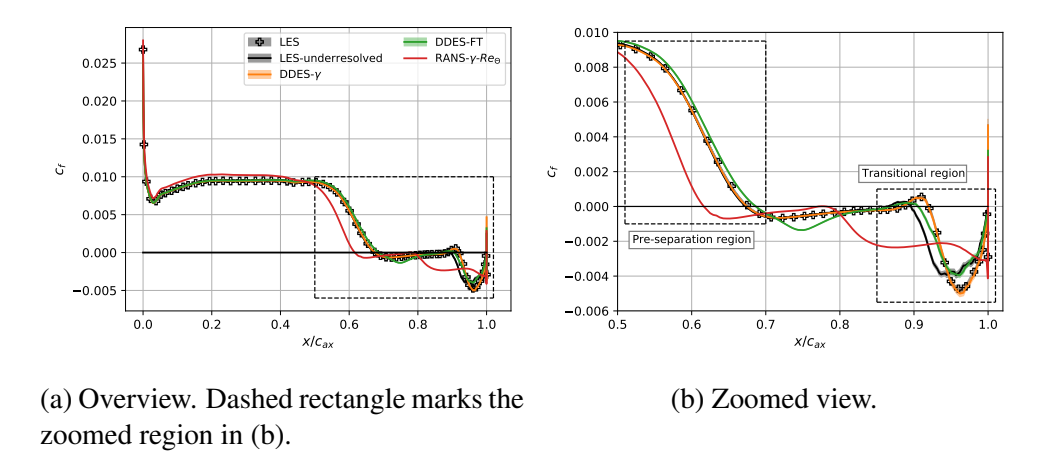
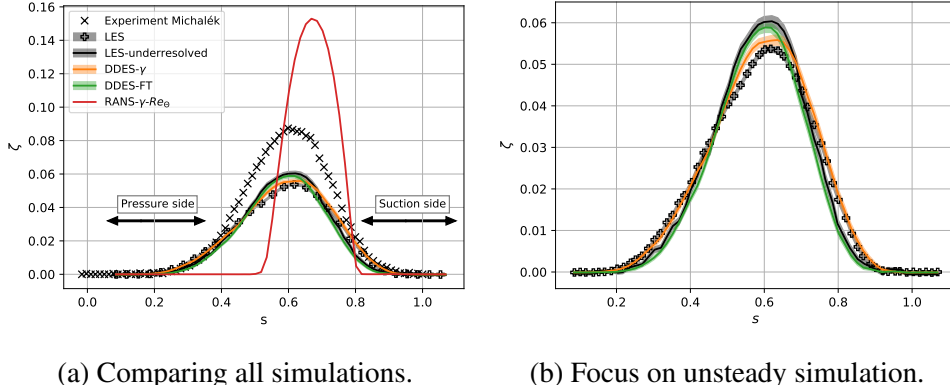


Figure 9: Friction coefficient along the suction surface including 95% confidence level for the unsteady simulations. Shown every 6^{th} point for LES reference data.

test case, the boundary layer profiles prior to separation were almost identical and differences only occurred in the separated shear layer, we can observe a different boundary layer development prior to separation without a transition model. Slightly higher c_f values for DDES-FT represent a 'more turbulent' boundary layer state resulting in a slightly delayed separation. The DDES- γ suppresses this undesired modelled turbulent content prior to the separation which emphasizes the necessity of a coupled DDES- γ model.

Besides the improved prediction of friction coefficient (cf. Fig. 9) and separation behavior by DDES- γ , a general potential of DDES approaches is also seen in the prediction of total pressure losses in the wake, since the model is capable to resolve the relevant turbulent structures in this region. These losses can be defined as $\zeta(s) = 1 - p_t(s)/p_{t1}$ with the relative pitchwise coordinate s, the total area-averaged inlet pressure over the inlet panel and the respective total pressure at each pitchwise position. Comparing these losses in Fig. 10 further verifies the beneficial behavior of the proposed DDES- γ model. RANS- γ - Re_{θ} clearly fails to predict the wake losses with a massive over-prediction of maximum losses and losses peak location. Focusing on the unsteady simulation in Fig. 10b illustrates the improvement of coupling DDES and γ -model. The over-prediction of maximum losses is reduced by DDES- γ while we see the overall best agreement between LES and DDES- γ . The improved prediction of the transition process (cf. Fig. 9) on the suction surface results in more accurate prediction of the losses on this side. A comparison with experimental data also shows good agreement in maximum peak location, meanwhile the overall maximum level is not met by any unsteady simulation result. Potential reasons for this are controversially discussed in the research community. One could be three-dimensional effects which affect the experimental results and are not captured by the periodic numerical setup. Another aspect is discussed by Bergmann et al. (2021). The different averaging procedure by experimental data acquisition and numerical analysis has also an effect on the actual wake losses. Overall, the experiment serves more as an orientation at this point. A comparison between LES and DDES illustrates the acceptable predictive quality of DDES- γ .



(b) Focus on unsteady simulation.

Figure 10: Wake losses at $x/c_{ax}=1.465$ (plane marked in Fig. 7) including 95 % confidence level for the unsteady simulations. Shown every 2nd point for LES reference data.

CONCLUSIONS

We introduced a coupling of the DDES with the γ -transition model. The effectiveness of this developed hybrid RANS/LES transition model was illustrated by two test cases. For the Volino series, we compare DDES results with experiments, RANS results and a numerical LES reference. Initially, three sub-grid models are considered. Based on the specific test case behavior, we further assessed the coupled DDES- γ exemplarily with Mockett's sub-grid length scale approach Δ_{ω} . The strengths of our proposed model are well documented, while the disruptive impact of the additional production term P_k^{\lim} (proposed in the original γ -model) and the failure of a fully turbulent DDES model are also illustrated. It was found, that a delay of producing modelled turbulent kinetic energy promotes a better prediction of the transitional process, which is supported by the coupling with the γ -transition model. General mechanisms of the coupled DDES- γ model could be explained with the Volino series and the beneficial behavior is presented in detail.

After analyzing a basic test case to explain the fundamental idea of our model coupling, we focus on a turbomachinery test case, namely T106C turbine cascade. Therefore, we compared an under-resolved LES, DDES- γ and a fully turbulent DDES on the same mesh with an additional LES reference on a fine mesh. The overall beneficial behavior of our DDES- γ was confirmed throughout all considered results whereas the fully turbulent DDES shows relevant deviations. The necessity of a transition model, ensuring a laminar boundary layer prior to the separation got clear and emphasize the requirement of an effective DDES- γ to predict separation-induced transition reliably.

Both test case analyses revealed, that reducing modelled turbulent kinetic energy, produced by the underlying RANS model, is essential to predict separation-induced transition. The sufficient development of resolved scales supports to capture this process, which is enabled by the delayed production of modelled eddy-viscosity. Since we now focused on the assessment of separation-induced transition with DDES- γ , the next step must be an assessment of bypass wake-induced transition mechanisms by DDES- γ .

ACKNOWLEDGEMENTS

We thank Prof. Ralph Volino for the very helpful support regarding his conducted experiments. The supply of comprehensive measurement data and the belonging measurement report is a valuable contribution for the first assessment of our proposed DDES- γ model with the Volino series. Our exchange helped to rank upcoming issues with numerical results and to put them into relation with experimental reference data. This research did not receive any specific grant from funding agencies in the public, commercial, or non-for-profit sectors. All simulations were carried out on DLR's supercomputer CARA³ within the internal DLR project ADaMant⁴.

REFERENCES

- Alam, M., Walters, D., and Thompson, D. (2013). A transition-sensitive hybrid RANS/LES modeling methodology for CFD applications. 51st AIAA Aerospace Sciences Meeting including the New Horizons Forum and Aerospace Exposition.
- Bergmann, M., Morsbach, C., Ashcroft, G., and Kügeler, E. (2021). Statistical error estimation methods for engineering-relevant quantities from scale-resolving simulations. *Journal of Turbomachinery*, 144(3).
- Chauvet, N., Deck, S., and Jacquin, L. (2007). Zonal detached eddy simulation of a controlled propulsive jet. *AIAA Journal*, 45(10):2458–2473.
- Hodara, J. and Smith, M. (2017). Hybrid Reynolds-averaged Navier-Stokes/large-eddy simulation closure for separated transitional flows. *AIAA Journal*, 55(6):1948–1058.
- Kim, W.-W. and Menon, S. (1999). An unsteady incompressible navier-stokes solver for large eddy simulation of turbulent flows. *International Journal for Numerical Methods in Fluids*, 31(6):983–1017.
- Langtry, R., Gola, J., and Menter, F. (2006). Predicting 2D airfoil and 3D wind turbine rotor performance using a transition model for general CFD codes. In *44th AIAA Aerospace Sciences Meeting and Exhibit*. American Institute of Aeronautics and Astronautics.
- Langtry, R. B. and Menter, F. R. (2009). Correlation-based transition modeling for unstructured parallelized computational fluid dynamics codes. *AIAA Journal*, 47(12):2894–2906.
- Menter, F., Kuntz, M., and Langtry, R. (2003). Ten years of industrial experience with the SST turbulence model. *Turbulence, Heat and Mass Transfer*, 4.
- Menter, F. R., Langtry, R. B., Likki, S. R., Suzen, Y. B., Huang, P. G., and Völker, S. (2006). A correlation-based transition model using local variables—part I: Model formulation. *Journal of Turbomachinery*, 128(3):413.
- Menter, F. R., Smirnov, P. E., Liu, T., and Avancha, R. (2015). A one-equation local correlation-based transition model. *Flow, Turbulence and Combustion*, 95(4):583–619.
- Michálek, J., Monaldi, M., and Arts, T. (2012). Aerodynamic performance of a very high lift low pressure turbine airfoil (T106C) at low reynolds and high mach number with effect of free stream turbulence intensity. *Journal of Turbomachinery*, 134(6).

³https://www.top500.org

⁴https://www.dlr.de/as/en

- Mockett, C., Fuchs, M., Garbaruk, A., Shur, M., Spalart, P., Strelets, M., Thiele, F., and Travin, A. (2015). Two non-zonal approaches to accelerate RANS to LES transition of free shear layers in DES. In *Progress in Hybrid RANS-LES Modelling*, pages 187–201. Springer International Publishing.
- Morsbach, C. and Bergmann, M. (2020). Critical analysis of the numerical setup for the large-eddy simulation of the low-pressure turbine profile T106C. In *ERCOFTAC Series*, pages 343–348. Springer International Publishing.
- Nürnberger, D. and Greza, H. (2002). Numerical investigation of unsteady transitional flows in turbomachinery components based on a RANS approach. *Flow, Turbulence and Combustion*, 69(3/4):331–353.
- Pasquale, D. D., Rona, A., and Garrett, S. (2009). A selective review of transition modelling for CFD. In *39th AIAA Fluid Dynamics Conference*. American Institute of Aeronautics and Astronautics.
- Qiu, S. and Simon, T. W. (1997). An experimental investigation of transition as applied to low pressure turbine suction surface flows. In *Volume 1: Aircraft Engine; Marine; Turbomachinery; Microturbines and Small Turbomachinery*. American Society of Mechanical Engineers.
- Shur, M. L., Spalart, P. R., Strelets, M. K., and Travin, A. K. (2015). An enhanced version of DES with rapid transition from RANS to LES in separated flows. *Flow, Turbulence and Combustion*, 95(4):709–737.
- Sørensen, N. N., Bechmann, A., and Zahle, F. (2011). 3D CFD computations of transitional flows using DES and a correlation based transition model. *Wind Energy*, 14(1):77–90.
- Spalart, P., Jou, W.-H., Strelets, M., and Allmaras, S. (1997). Comments on the feasability of LES for wings, and on a hybrid RANS/LES approach. *Computer Science*.
- Spalart, P. R., Deck, S., Shur, M. L., Squires, K. D., Strelets, M. K., and Travin, A. (2006). A new version of detached-eddy simulation, resistant to ambiguous grid densities. *Theoretical and Computational Fluid Dynamics*, 20(3):181–195.
- Strelets, M. (2001). Detached eddy simulation of massively separated flows. In *39th Aerospace Sciences Meeting and Exhibit*. American Institute of Aeronautics and Astronautics.
- Suzen, Y. B., Huang, P. G., Hultgren, L. S., and Ashpis, D. E. (2003). Predictions of separated and transitional boundary layers under low-pressure turbine airfoil conditions using an intermittency transport equation. *Journal of Turbomachinery*, 125(3):455–464.
- Travin, A., Shur, M., Strelets, M., and Spalart, P. R. (2002). Physical and numerical upgrades in the detached-eddy simulation of complex turbulent flows. In *Fluid Mechanics and Its Applications*, pages 239–254. Springer Netherlands.
- Tucker, P. (2013). Trends in turbomachinery turbulence treatments. *Progress in Aerospace Sciences*, 63:1–32.

- Tyacke, J., Tucker, P., Jefferson-Loveday, R., Vadlamani, N. R., Watson, R., Naqavi, I., and Yang, X. (2013). Large eddy simulation for turbines: Methodologies, cost and future outlooks. *Journal of Turbomachinery*, 136(6).
- Volino, R. (2002). Measurements in separated and transitional boundary layers under low-pressure turbine airfoil conditions. Technical report, NASA Glenn Research Center.
- Volino, R. J. and Hultgren, L. S. (2000). Measurements in separated and transitional boundary layers under low-pressure turbine airfoil conditions. *Journal of Turbomachinery*, 123(2):189– 197.
- Walters, D. K. and Cokljat, D. (2008). A three-equation eddy-viscosity model for Reynolds-averaged Navier–Stokes simulations of transitional flow. *Journal of Fluids Engineering*, 130(12).
- Wang, L. and Fu, S. (2009). Modelling flow transition in a hypersonic boundary layer with reynolds-averaged navier-stokes approach. *Science in China Series G: Physics, Mechanics and Astronomy*, 52(5):768–774.
- Wang, L., Fu, S., Carnarius, A., Mockett, C., and Thiele, F. (2012). A modular RANS approach for modelling laminar–turbulent transition in turbomachinery flows. *International Journal of Heat and Fluid Flow*, 34:62–69.
- Xiao, Z., Wang, G., Yang, M., and Chen, L. (2019). Numerical investigations of hypersonic transition and massive separation past orion capsule by DDES-tr. *International Journal of Heat and Mass Transfer*, 137:90–107.
- Yanaoka, H., Inamura, T., and Kobayashi, R. (2007). Numerical simulation of separated flow transition and heat transfer around a two-dimensional rib. *Heat Transfer—Asian Research*, 36(8):513–528.
- Yin, Z., Ge, X., and Durbin, P. (2021). Adaptive detached eddy simulation of transition under the influence of free-stream turbulence and pressure gradient. *Journal of Fluid Mechanics*, 915.